Long-range Universality and Chaos in Ultracold Collisions of the Highly Magnetic Atoms

Svetlana Kotochigova,

Temple University, Physics Department

INT Program, April 24, 2014

Universality in Few-Body Systems: Theoretical Challenges and New Directions

Collaborators:

Francesca Ferlaino's group	University of Innsbruck
Eite Tiesinga	NIST, JQI

Temple U. team

Kostas Makrides

Alexander Petrov

Collisions of ground state cold atoms

Van-der-Waals (contact) interactions

$$V(R) = -\frac{C_6}{R^6} \longrightarrow V(R) = \frac{4\pi\hbar^2}{m} a_S \delta(R)$$

Short range and isotropic,
does *not* depend on angle of approach

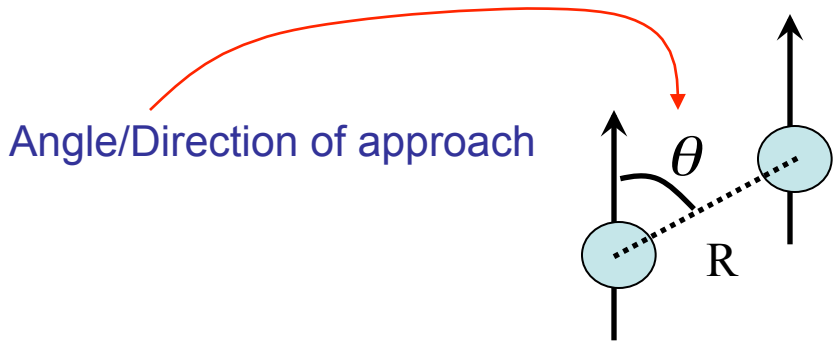

(magnetic) dipole-dipole interactions

$$V_{dd} = \frac{\mu_0}{4\pi} S^2 \left(g_J \mu_B\right)^2 \left(1 - 3\cos^2(\theta)\right) \frac{1}{R^3}$$

Long range and anisotropic,
does depend on angle of approach

Different dipolar systems

« Magnetic atoms »

$d = 1\,\mu_B$ to $10\,\mu_B$

Rb, Cr, Dy, and Er

Dipole-dipole interaction

smaller

$\times \alpha^2 = \frac{1}{137^2}$

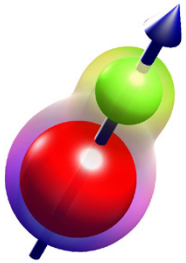

Hetero-nuclear molecule with (field induced-) electric dipole moment

$d \approx ea_0$

KRb and RbCs

larger

$\times n^4 = 10^8$

Rydberg atoms

$d = n^2 ea_0$

Mostly Rb

High-spin atomic systems

Experimental realization of strongly-correlated quantum gases:

Cr	Griesmaier et al. (PRL 94, 160401 (2005))
Dy	Lu et al. (PRL 107, 190401 (2011))
Er	Aikawa et al. (PRL 108, 210401 (2012))

Over the last ten years experimental advances have lead to better control of degenerate gases of magnetic ^{52}Cr in the $^{7}S_3$ ground state. These atoms have a large magnetic moment of 6 μ_B.
Developments started at the University of Stuttgart in the group of Prof. Pfau. A Bose-Einstein condensate (BEC) of Cr atoms was reported in 2005.

Researchers from the University of Illinois and Stanford University in the group of Prof. B. Lev, have formed the BEC of the bosonic ^{164}Dy atoms at temperature below 30 nK.

The group of Prof. Ferlaino at the University of Innsbruck have prepared a BEC of bosonic ^{168}Er atoms, followed by the creation of quantum gases of other bosonic isotopes as well the sole fermionic isotope ^{167}Er.

Dipole-dipole spin dynamics

Dipole-dipole interactions lie at the heart of the complex spin dynamics observed with Cr in optical lattice.

In experiments of T. Pfau and B. Laburthe-Tolra

Spontaneous magnetization by lowering temperature:

BEC in magn. sublevel distribution

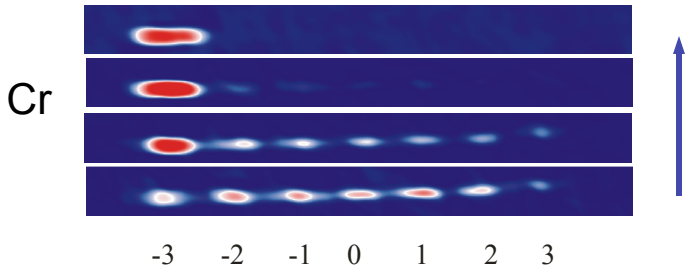

B. Laburthe-Tolra group, PRL **108**, 045307 (2012)

Spin dynamics couples the spin degree of freedom to orbital momentum of the relative motion due to anisotropy.

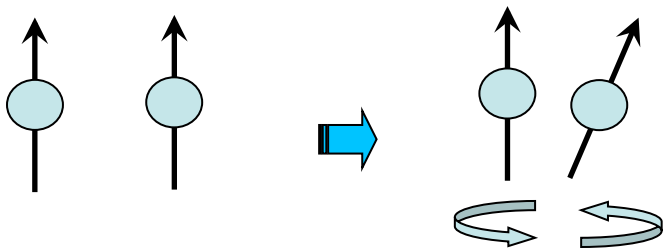

L. Santos and T. Pfau, PRL **96**, 190404 (2006)

A. Petrov, E. Tiesinga, and S. Kotochigova, PRL **109**, 103002 (2012)

Applications in an optical lattice

Quantum magnetism in optical lattices

(without spatial disorder and with ability to tune interactions)

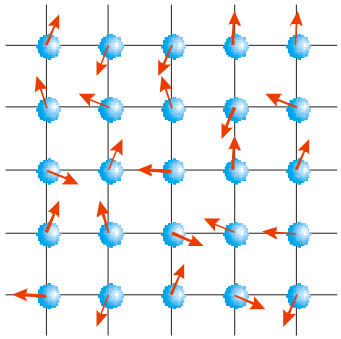

Exotic many-body phases known as supersolids, liquid crystals, and quantum ferrofluids could be created

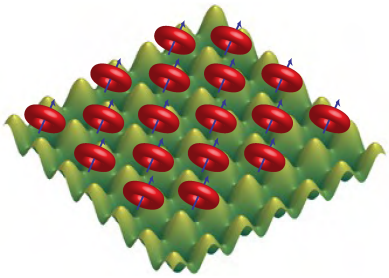

B. M. Fregoso et al. New J. Phys. 11, 103003 (2009)

Application in Quantum Computing

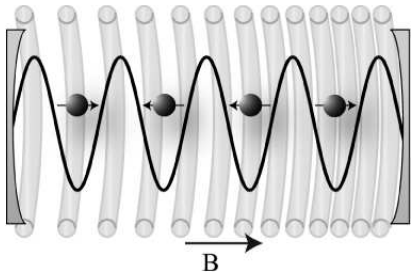

The long range character of dipole-dipole interaction can be used to entangle two or more atoms.

A. Derevianko & C. Cannon, PRA **70**, 062319 (2004)

Outline

- Here we explore the dipolar nature of FRs in interactions of highly magnetic atoms, such as Dysprosium (Dy) and Erbium (Er) atoms.

- First, we perform calculation of realistic properties of the interaction potentials between the atoms.

- Based on an exact close-coupling model we determine the likelyhood of resonances and their density as a function of magnetic field.

- We perform RMT analyses of the distribution of magnetic field separations between neighboring Feshbach resonances and compare to similar analyses of the experimental data.

- In parallel, we develop random quantum defect theory to estimate mean resonance densities as a function of partial wave.

- We analyze and identify low B-field FRs observed in the experiments with Er, calculate and explain measured magnetic moments values.

Dysprosium and Erbium

Dysprosium has an unfilled $4f^{10}$ shell lying beneath a filled $6s^2$ shell leading to a large orbital, L = 6, and total, J = 8, angular momentum. Its ground $^5I_8$ state has a magnetic moment of $10\mu_B$.

Erbium has an unfilled $4f^{12}$ shell lying beneath a filled $6s^2$ shell leading to a large orbital, L = 5, and total, J = 6, angular momentum. Its ground $^3H_6$ state has a magnetic moment of $7\mu_B$.

Large magnetic moment is due to large number of unpaired electrons.

The electronic structure of non-S atom leads to additional source of anisotropy.

For a close-coupling calculation we needed all electronic potentials dissociating to two ground-state atoms. There are 153 for Dy_2 and 91 potentials for Er_2 dissociating to the atomic ground state limits.

Relativistic properties

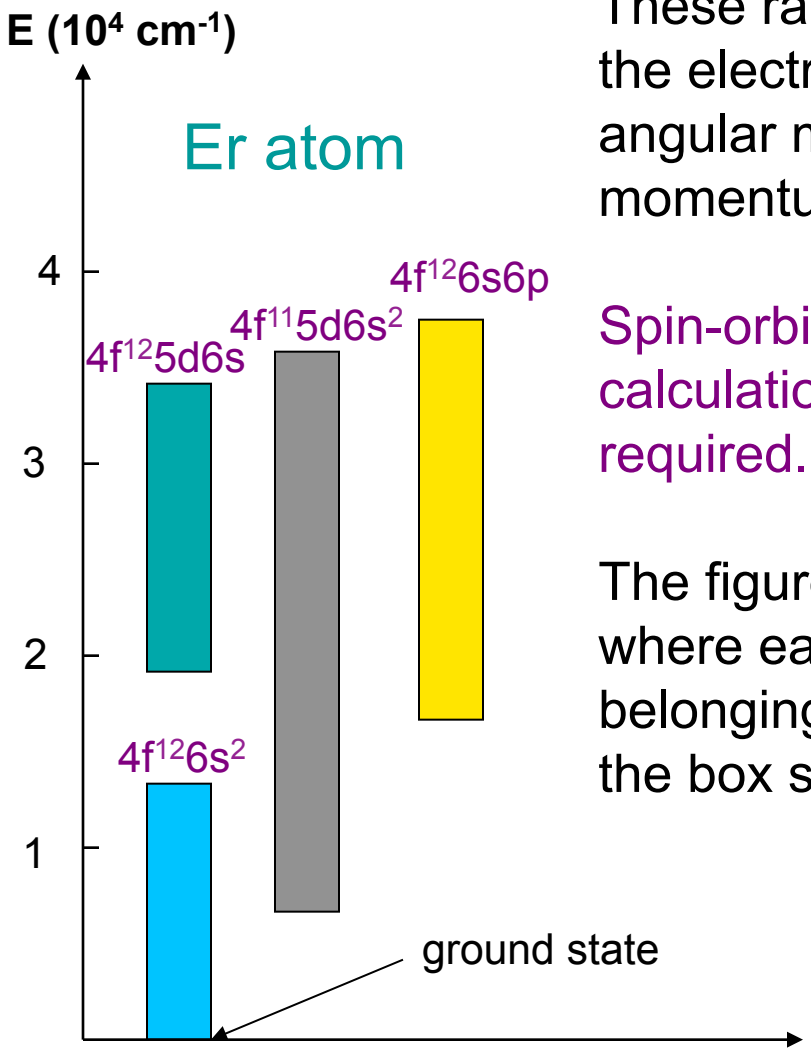

These rare-earth atoms have heavy nuclei, where the electron spin S is strongly coupled to the angular momentum L. Only the total angular momentum j and its projection m matter.

Spin-orbit splitting is very large and a relativistic calculation for the atom and the molecule is required.

The figure shows the excitation spectrum of Er, where each box describes groups energy levels belonging to the same configuration. The height of the box shows the spread due to spin-orbit effects.

Magnetic submerged 4f-shell atoms

The original expectation was that inelastic collisions of these atoms are suppressed.

Recent experiments by J. Doyle's group at Harvard U. show that inelastic rates for submerged-shell atoms are of the same order as for non-submerged-shell atoms.

A possible explanation is a strong anisotropy in the interactions.

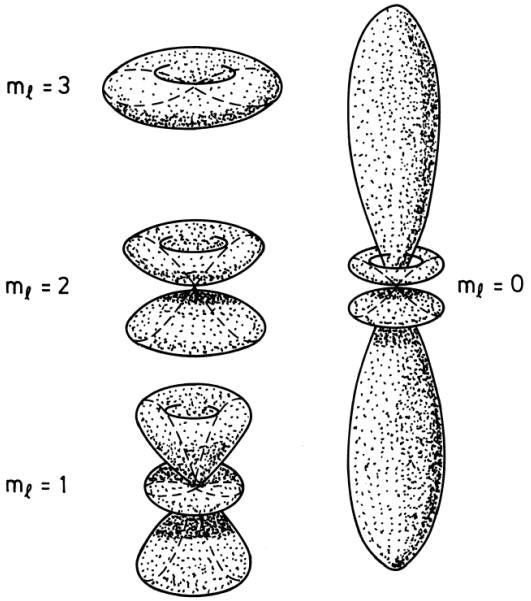

The angular variation of the 4f-wave functions.

When atoms approach each other from different directions. The interaction energy is different.

Long-range interaction potentials

There are three dominant long-range forces between magnetic atoms: magnetic dipole-dipole, dispersion, and electric quadrupole-quadrupole interaction.

The magnetic dipole-dipole interaction $\hat{V}_{\mu\mu} = \frac{\mu_0 (g_j \mu_B)^2}{4\pi} \frac{(\vec{j}_1 \cdot \vec{j}_2) - 3 j_{1z} j_{2z}}{R^3}$

projection z along internuclear axis

The dispersion interaction is

$$\hat{V}_{\mathrm{vdW}} = \frac{1}{R^6} \left\{ c^{(0)} \hat{I} + c^{(1)} \vec{j}_1 \cdot \vec{j}_2 + c^{(2)} (\vec{j}_1 \cdot \vec{j}_1 - 3 j_{1z}^2) + c^{(2)} (\vec{j}_2 \cdot \vec{j}_2 - 3 j_{2z}^2) + c^{(3)} (\vec{j}_1 \cdot \vec{j}_2 - 3 j_{1z} j_{2z}) + \cdots \right\}$$

isotropic contributions

anisotropic contributions

The electric quadrupole-quadrupole interaction is

$$\hat{V}_{QQ} = \frac{Q^2}{R^5} (\vec{j}_1 \cdot \vec{j}_1 - 3 j_{1z}^2) \otimes (\vec{j}_2 \cdot \vec{j}_2 - 3 j_{2z}^2)$$

Dispersion interactions

We use 2nd -order perturbation theory in the dipole-dipole interaction summing over many excited atomic states.

We derived the full vdW Hamiltonian (PCCP, **13**, 19165-70 (2011))

$$\langle (j_a j_b) J' \Omega | \frac{\hat{C}_6}{R^6} | (j_a j_b) J \Omega \rangle = \frac{1}{R^6} \sum_{\substack{j'_a j'_b \\ \text{exc. states}}} K_{j'_a j'_b} \; A^{j'_a j'_b}_{J' J}$$

where $A^{j'_a j'_b}_{J' J}$ are *independent* of atomic transition frequencies and dipole moments.

$K_{j'_a j'_b}$ is a symmetric matrix elements and obtained from atomic transition frequencies and oscillator strengths that are taken from experimental data.

In total, 62 for Dy and 38 for Er experimental atomic transitions from the ground state were used.

Adiabatic C_3 and C_6 coefficients for Dy+Dy

We need only consider gerade symmetry potentials as we will be studying the collision between spin-polarized bosonic atoms.

Arrows indicate the orientation of J

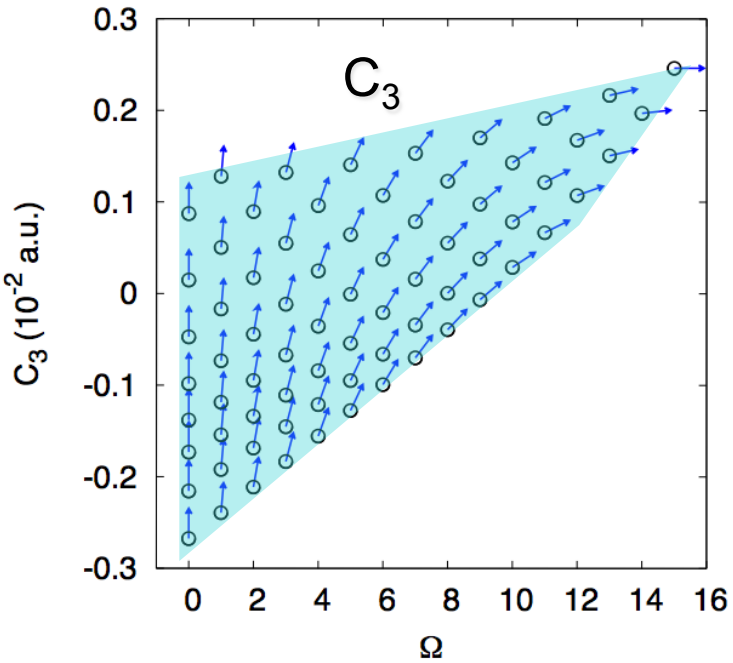

Values are both positive and negative.

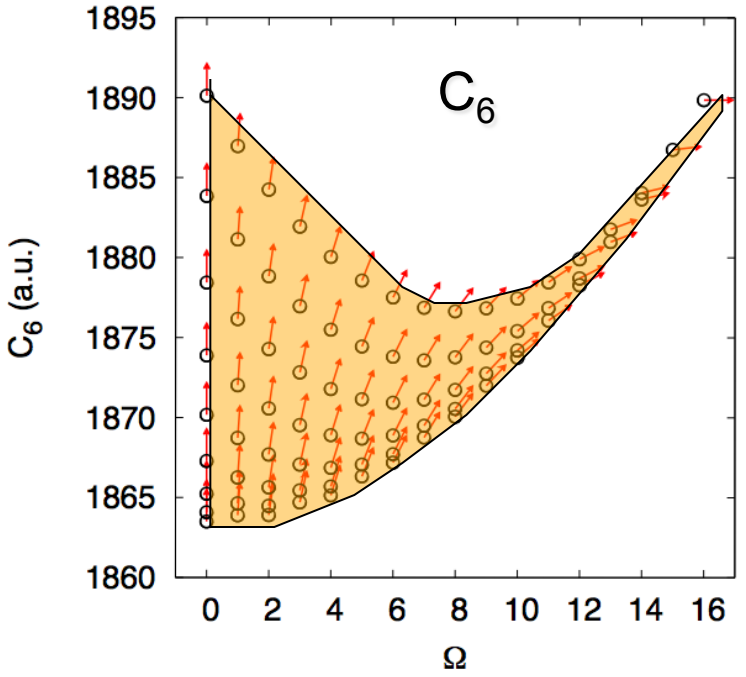

Positive values correspond to attractive potentials

81 gerade potentials dissociating to the Dy ($^5I_8$) + Dy ($^5I_8$) limit

S.K. and A. Petrov, PCCP 13, 19165 (2011)

Coefficients for Er+Er

We find adiabatic C_3 and C_6 coefficients by diagonalizing the matrix of the magnetic dip-dip and vdW dispersion operator for each Ω.

Ω is the projection of $j=j_a+j_b$ on internuclear axis.

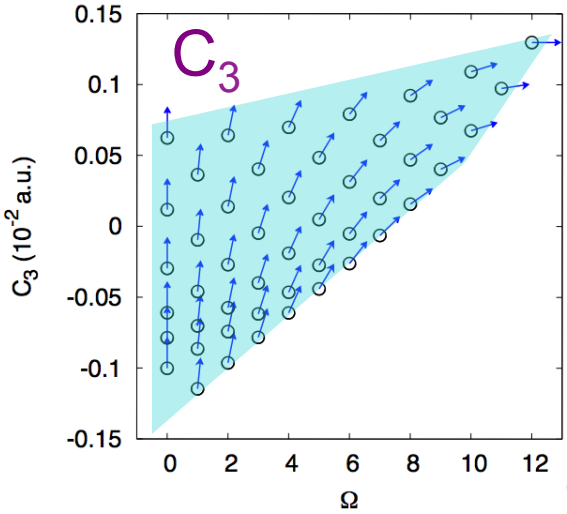

values are both positive and negative.

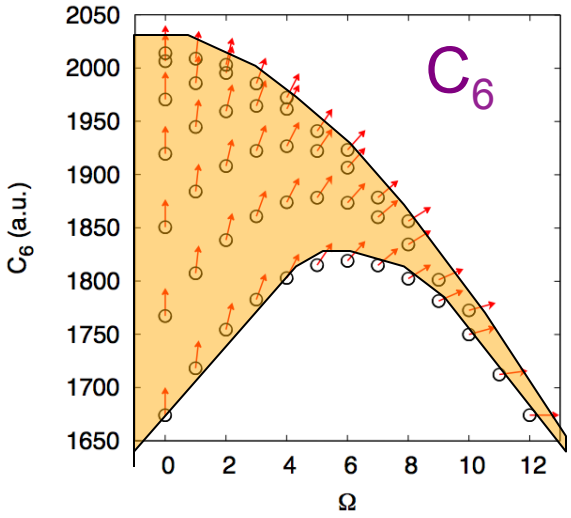

only attractive potentials.

48 *gerade* potentials

The anisotropic C_6 splitting is 10x smaller than the mean isotropic value.
(The anisotropy in Er is 10x larger than in Dy and is of opposite sign.)

Relative size of interactions in Er collisions

In addition to the three long-range interactions we need to consider the Zeeman interaction as well as the rotation of the molecule.

Zeeman, rotational, and (dominant) isotropic dispersion interactions can shift levels, but can not induce spin (m-projection) changes.

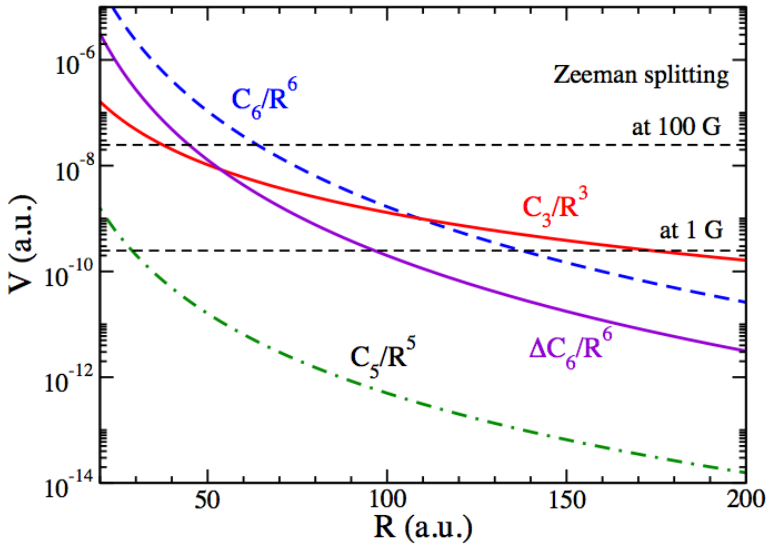

The magnetic dip.-dip., and anisotropic dispersion interactions lead to coupling between different Zeeman sublevels.

The quadrupole moment of Er atom in the ground state is small (+0.03 a.u.) therefore electronic quadrupole-quadrupole interaction can be safely ignored.

Details on short-range potentials of Er

For short-range we assume a potential operator with a tensor form that is the same as that for the dispersion potential but now with an R-dependent dispersion coefficient c_i. That is

$$V(R) = \sum_i c_i^*(R)\, C_{k_i}(\theta, \phi) \cdot T^i_{k_i}(j_a, j_b)$$

Operators containing atomic spins j_a and j_b

approaches $1/R^6$ for large R

Orientation dependence

The coefficients are determined from an accurate CCSD(T) calculation of the adiabatic electronic potentials $V_{\Omega=16}$ and $V_{\Omega=12}(R)$ and C_6 coefficients.

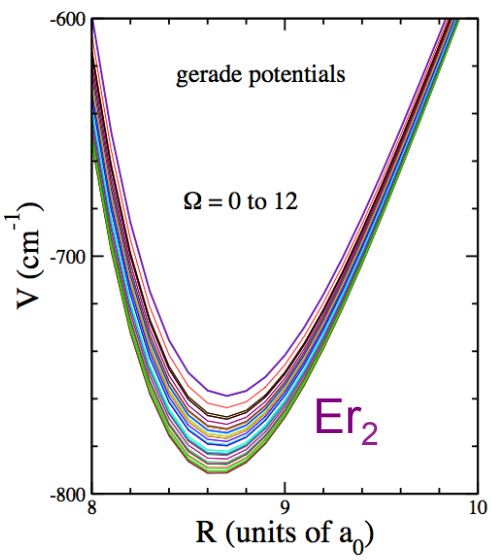

Typical numbers of quantum gases

Looking at the interaction of Dy and Er atoms in dipole traps.

Density : 10^{12} to 10^{15} at/cm^3 (10^{22} at/cm^3 for liquid He)

Interparticle distance ~ 100 nm

Temperature : 1 nK to 1μK

de Broglie wavelength > 100 nm (BEC occurs)

Short range isotropic atom-atom interactions are characterized by s-wave scattering length. The typical value is a_S ~ 5 nm.

It can be tuned via magnetic Feshbach resonances, which allow the scattering length to be increased leading to strongly interacting quantum gases.

Feshbach resonances

We can control interactions with Feshbach resonances (FR).

Atoms are prepared in the open channel.

In the course of the collision a coupling between closed and open channels can occur.

Varying magnetic field we can shift the closed channel energy with respect to open channel energy.

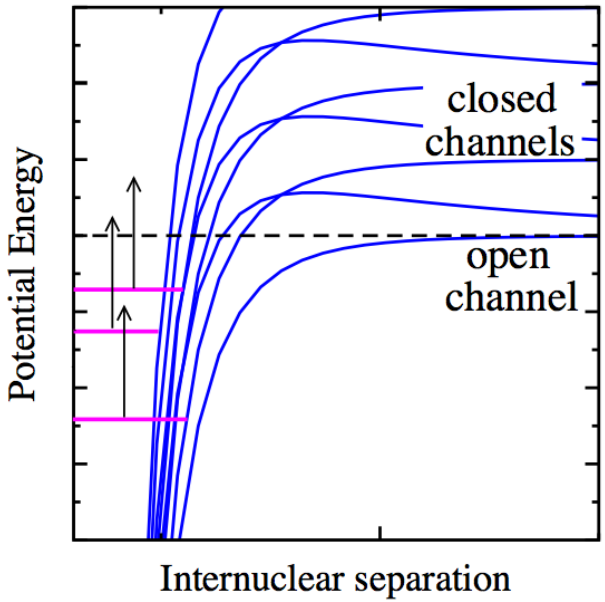

Schematic picture of interaction potentials

Resonances occur when bound states cross the threshold.
(To have FR we need at least two channels.)

Anisotropic nature of FRs

The nature of the FR in collisions of bosonic sub-merged shell atoms is different from that in alkali-metal atom collisions.

In AM the hyperfine interaction between electron and nuclear spins gives sufficient complexity so that Feshbach resonances appear without anisotropy.

The magnetic dipole-dipole interaction between alkali-metal atoms plays a lesser role, creating narrow FB resonances that are more difficult observable.

The nature of FB resonances in the interaction of magnetic atoms such as bosonic Dy and Er relies solely on the anisotropy.

This is a constructive effect of the anisotropy.

Useful properties of Feshbach resonances

- FR make it possible to convert a weakly interacting gas of atoms into one that is strongly interacting.

- FR are used to create BECs of weakly-bound molecules, which can be optically stabilized to deeply-bound molecules.

- Alternatively, interactions can be turned off altogether to create an ideal Fermi or Bose gas, for which thermodynamic properties are known analytically.

- For fermionic atoms, the phase transitions and universal many-body behavior of strongly interacting atoms can be studied via FR.

- Finally, three-body Efimov physics can be explored.

Close-coupling calculation

We have performed a first-principle coupled-channel calculation of Dy+Dy and Er+Er scattering in the basis

$$|j_a m_a, j_b m_b, \ell m_\ell\rangle \equiv Y_{\ell m_\ell}(\theta,\phi)|j_a m_a\rangle|j_b m_b\rangle$$

with projections m_a and m_b along the magnetic field direction.

In this basis Zeeman and rotational interactions are diagonal and coupling basis states is due to BO potentials and anisotropic long-range forces.

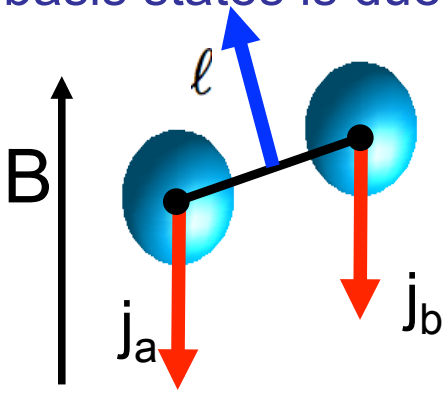

For Er and Dy atoms in the lowest stretched state with $m_{a,b} = -6$ and $m_{a,b} = -8$ we find that for *s*-wave (*l*=0) collisions there is only one *s*-wave channel since

$M_{total} = m_a + m_b + m_l = -12$ (-16) is conserved.

vibration rotation Born-Oppenheimer

$$H = -\frac{\hbar^2}{2\mu_r}\frac{d^2}{dR^2} + \frac{\vec{\ell}^2}{2\mu_r R^2} + H_Z + V(\vec{R},\tau)$$

Zeeman interaction

Long-range potential energy curves for ^{164}Dy+^{164}Dy collisions.

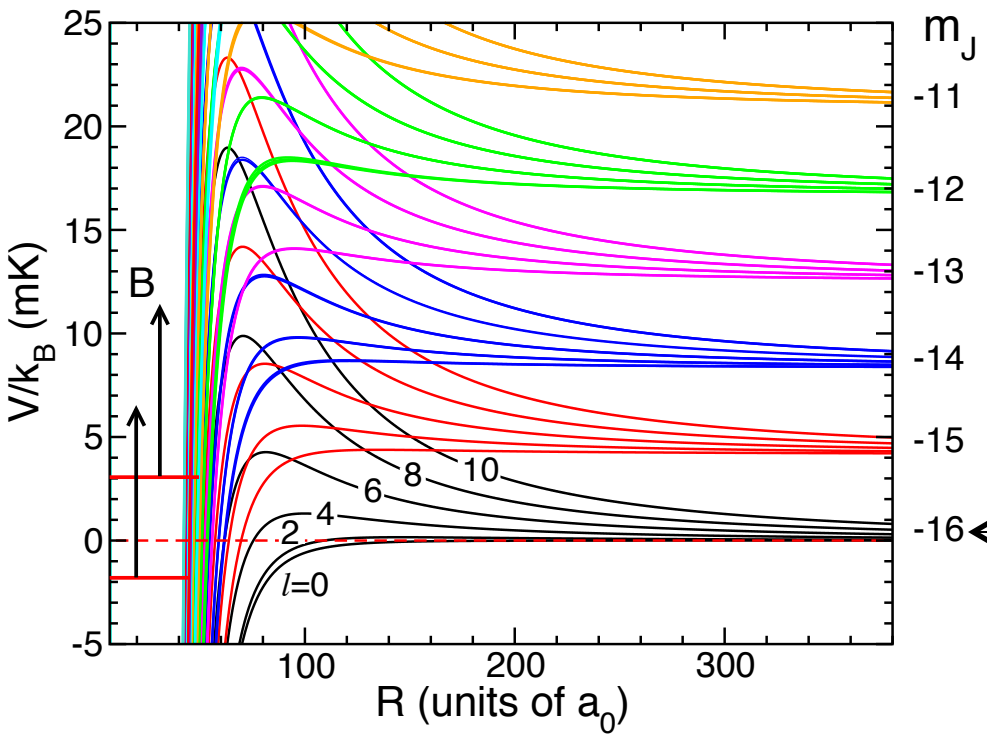

Graph shows the 91 diabatic channels.

B = 50 G L_{max} = 10

For bosonic Dy and Er there is no nuclear hf structure and for large R only the Zeeman splitting is present.

Dipolar FRs for Dy+Dy

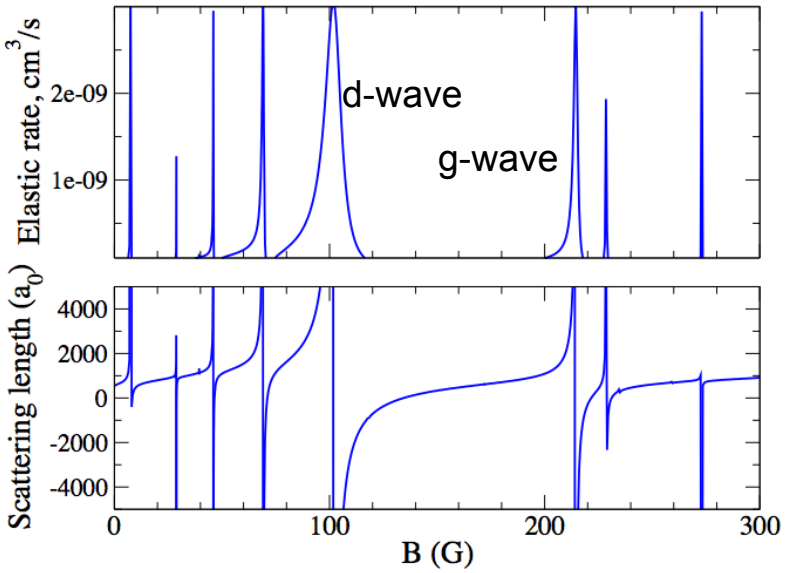

^{164}Dy + ^{164}Dy, E = 30 nK

partial waves upto 10

A. Petrov, E. Tiesinga, and S. K., PRL **109**, 103002 (2012)

K. Baumann et al. PRA 89, 020701® (2014)

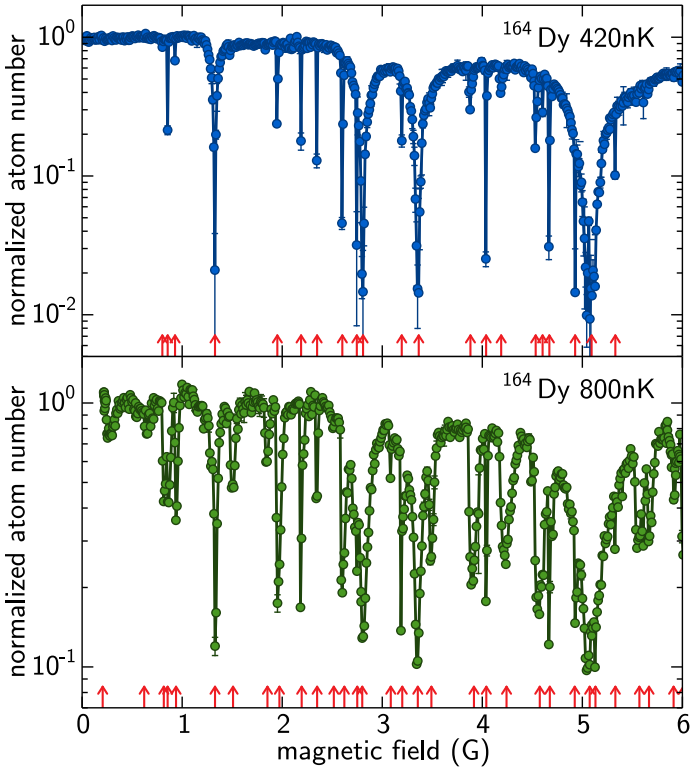

It seems likely that Dy is more anisotropic than previously thought.

In addition, at higher temperatures around 400-800 nK non-zero partial wave collisions may become important and increase the resonance density.

Effect of anisotropy

^{164}Dy + ^{164}Dy E/k = 30 nK M_{tot} = -16

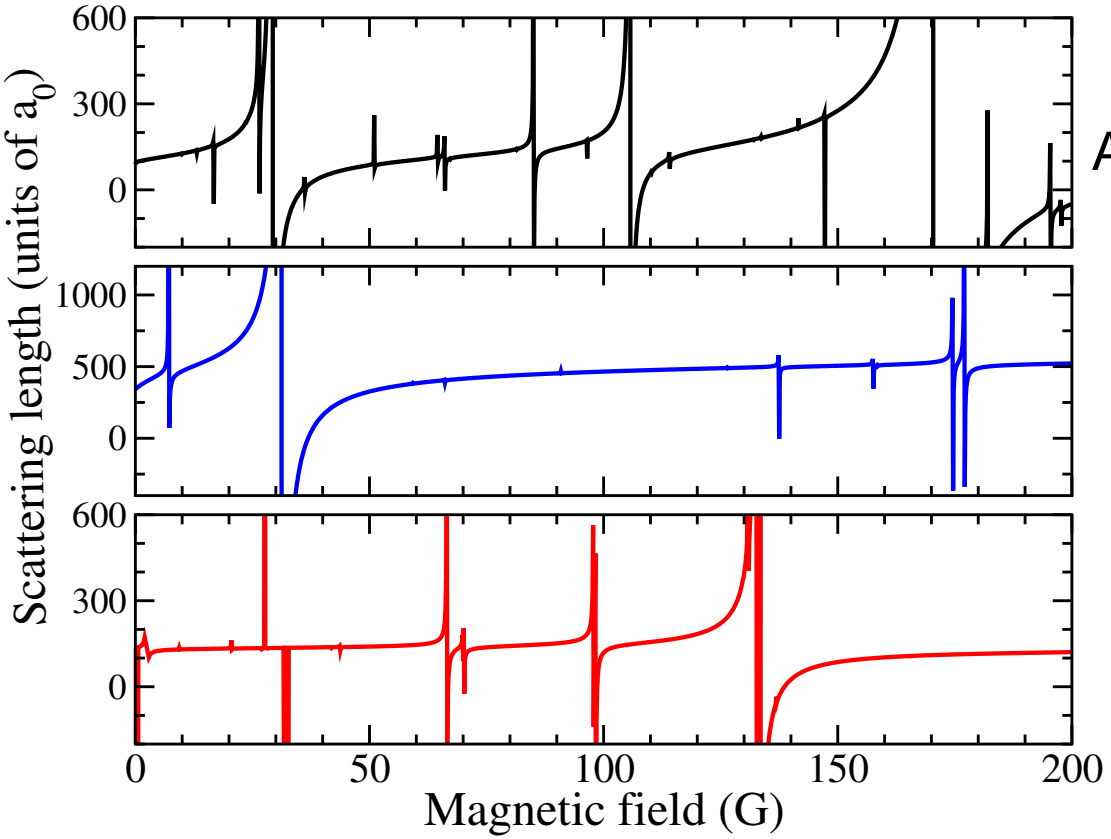

All anisotropies are included

No anisotropy in dispersion

No dipole-dipole interaction

Dipolar FRs for Er+Er

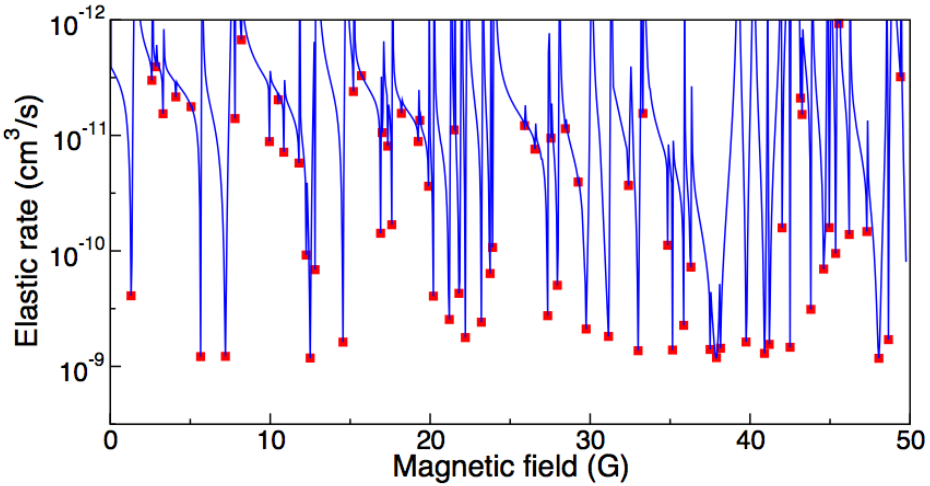

^{168}Er+^{168}Er

E/k=360 nK; M_{total} = -12
partial waves up to L_{max}=20

We obtain a large number overlapping resonances

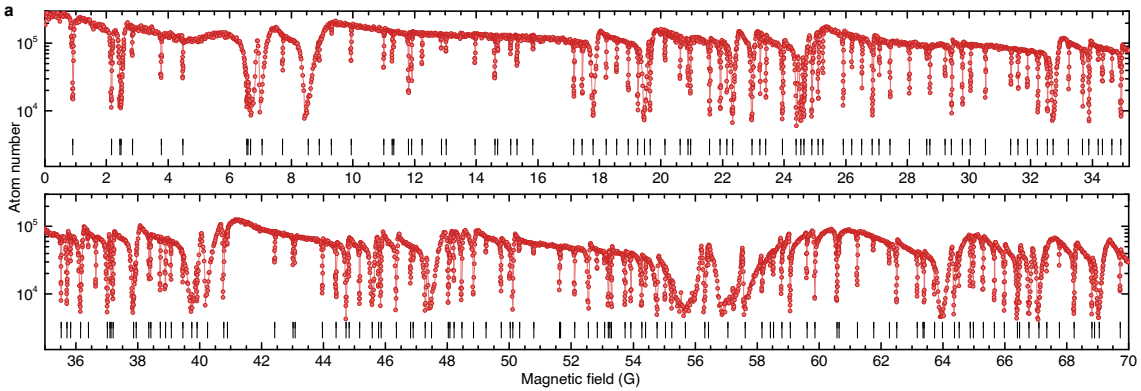

^{168}Er+^{168}Er

Experimental spectrum by group of F. Ferlaino

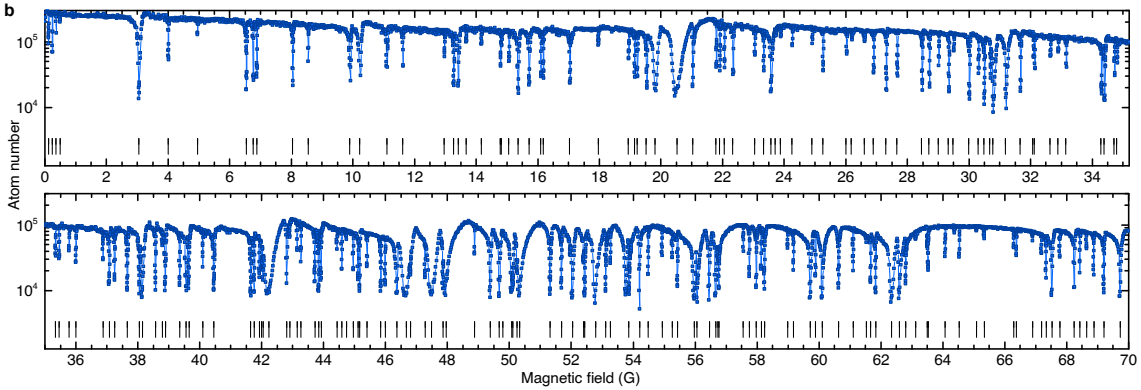

^{166}Er + ^{166}Er

Feshbach resonances for $^{166}Er+^{166}Er$

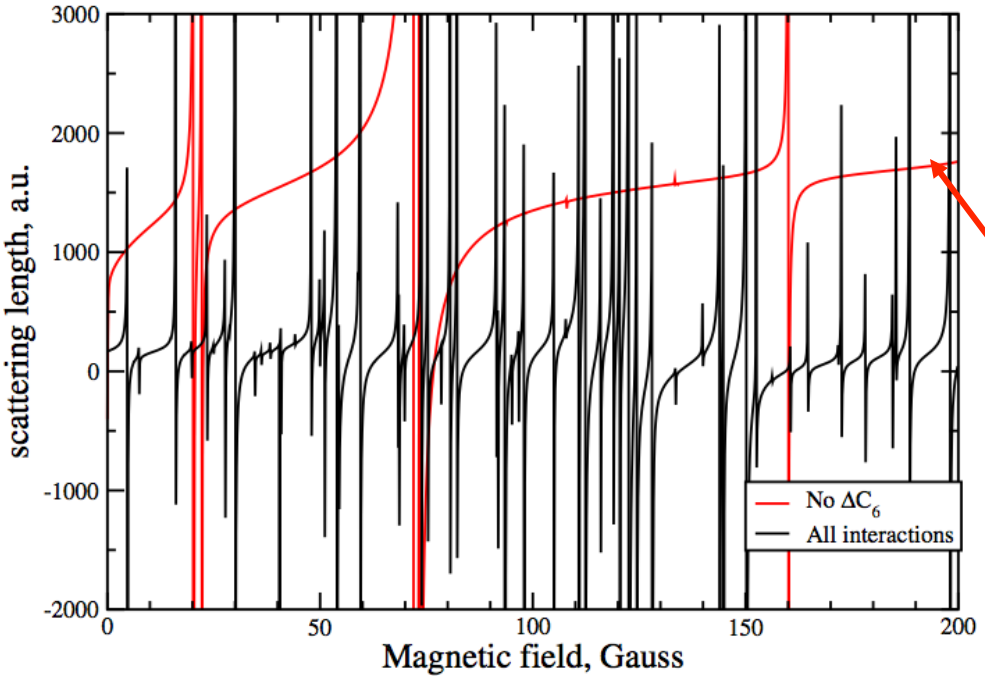

The anisotropic dispersion is switched off.

Notice disappearance of most resonances.

The resonance positions change dramatically if we vary the depth of the Ω=12 potential by just a few cm^{-1}, well within the uncertainty of our calculation.

This change of depth automatically modifies those of all other potentials.

Chaotic behavior of FRs

A quantitative reproduction of the experimental spectra requires precise knowledge of all gerade short-range potentials, which are currently unavailable.

We can, however, perform a RMT analyses of the distribution of magnetic field separations between neighboring Feshbach resonances and compare to similar analyses of the experimental data.

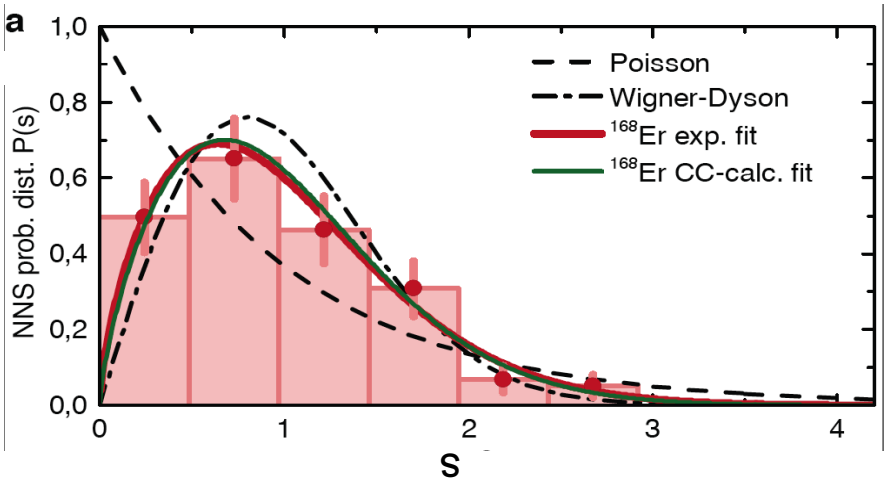

Nearest neighbour spacing (NNS)

S = NNS/mean separation

Brody distribution is a good fit.

Close-coupling data are obtained from calculation with even partial waves up to 20.

A. Frisch *et al*. Nature, vol. 507, 475 (2014)

Random QTD

We developed an analytical random quantum defect theory to estimate the mean resonance density for larger L_{max}.

First, we estimate the energy interval Δ where the last bound state of each BO potential must occur. This interval increases rapidly with partial wave and can be expressed in terms of the isotropic C_6.

Since the short-range potentials are not accurately known, we assume equal probability of finding a bound state in this interval.

$\Delta/E_{vdW} \sim 38.7 + 25.5l + 3.17l^2$

Zeeman energy of bound state changes as $E_b + g\mu_B \Delta m\, B$

For each part. wave we have a FR in B-field interval from 0 to $B_{max} = \Delta/(g\mu_B \Delta m)$

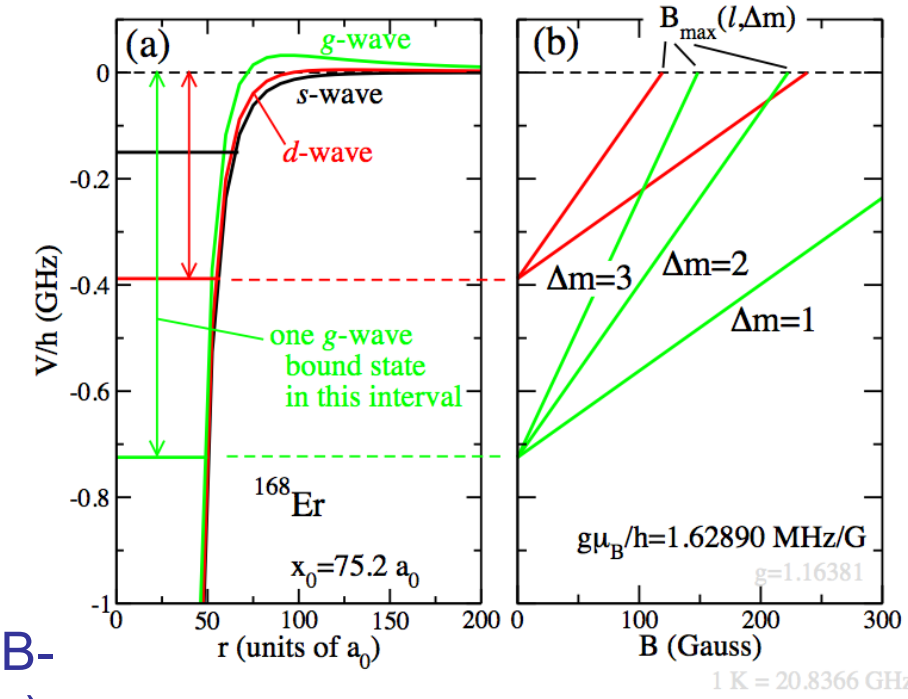

Close-coupling vs RQDT

Mean resonance density as a function of largest included partial wave.

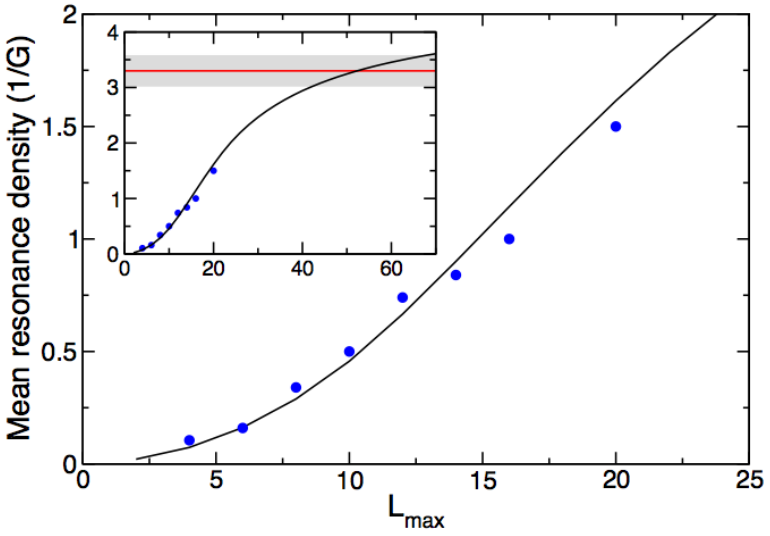

The black solid curve corresponds to an estimate of mean density using RQDT.

It seems to converge because the size of bin changes as L^2_{max} while the number of channels goes as L_{max}

The blue markers represent results from numerical close-coupling calculations when we systematically increase L_{max}.

The inset shows the same data up to L_{max}= 70 as well as the experimental measurement of the mean resonance density (red line and one-sigma uncertainty indicated by gray region)

RQDT suggests that to explain the experimental mean resonance density we need to include at least 60 partial waves in a cc calculation.

A. Frisch *et al*. Nature, vol. 507, 475 (2014)

Magnetic moments of ^{168}Er FRs

F. Ferlaino's FB measurement of magnetic moments.

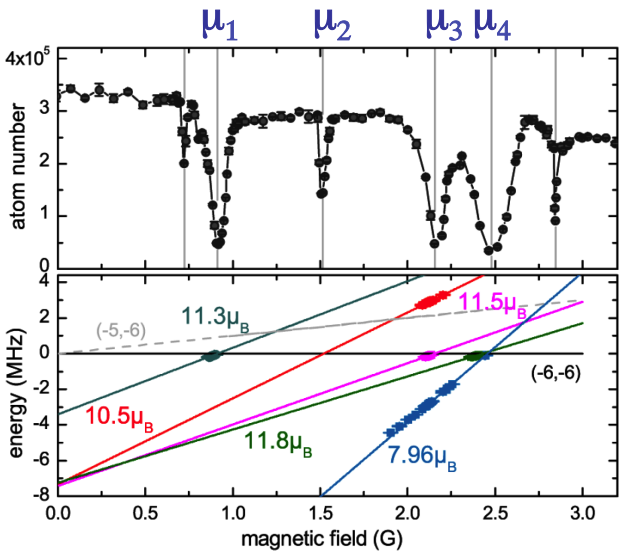

They used magnetic-field modulation spectroscopy to measure binding energies of Feshbach molecules as a function of B to provide values of μ for the strongest Feshbach resonances shown on this graph.

Our first attempt to analyze these FRs and calculate their magnetic moments.

a) calculate the adiabatic potentials versus R for a magnetic field.

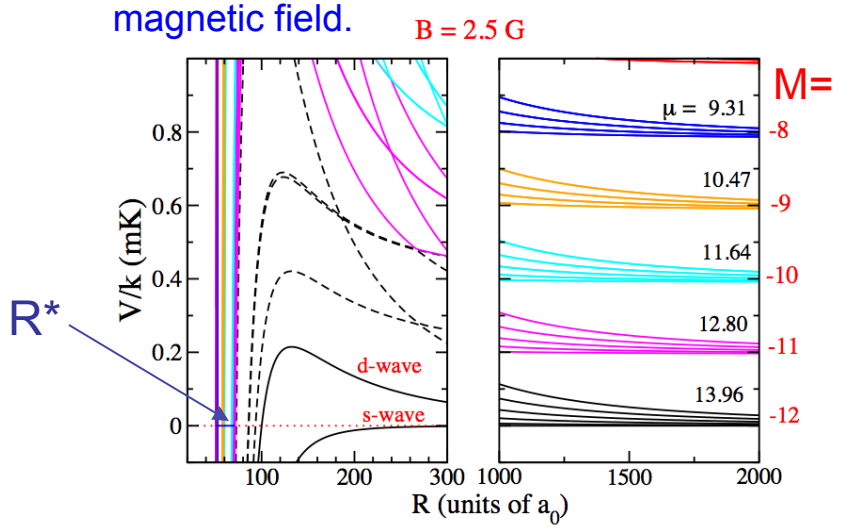

b) Assume that a resonance is due to *one* closed-channel adiabat.

c) Outer turning point R* of this adiabat at energy of entrance channel. I.e. $V_{closed}(R^*)=0$

d) Magnetic moment is given $\mu(R^*) = -dV_{closed}(R^*)/dB$

$$\mu(R^*) = \sum_{JM\ell m} (g\mu_B M)|c_{JM\ell m}(R^*)|^2$$

Linear combination of magnetic moments of diff. Zeeman sublevels

Magnetic moments Continued

We find that these "adiabatic" magnetic moments converge quickly with number of partial waves and only weakly depend on the strength of the isotropic and anisotropic dispersion potentials.

B = 2.5 G

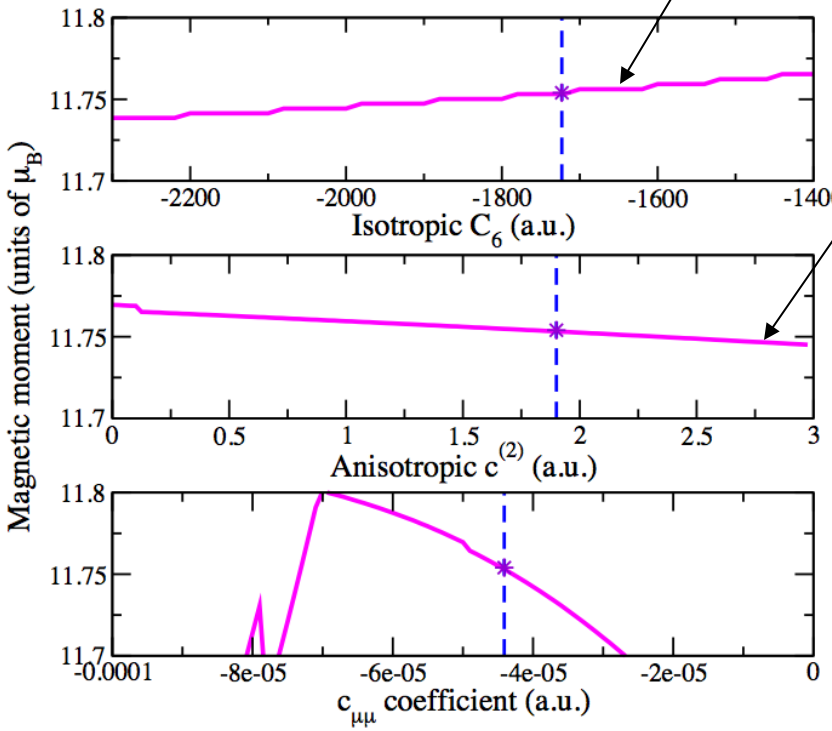

FR at 2.5 G

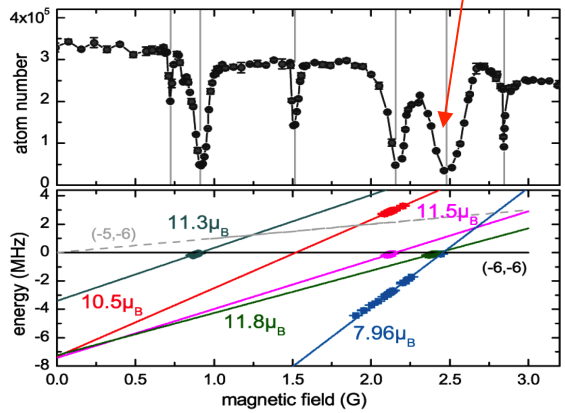

It does depend on the magnetic dipole-dipole interaction!

$$\hat{V}_{\mathrm{vdW}} = \frac{1}{R^6}\left\{c^{(0)}\hat{I} + c^{(1)}\vec{j}_1\cdot\vec{j}_2 + c^{(2)}(\vec{j}_1\cdot\vec{j}_1 - 3j_{1z}^2) + c^{(2)}(\vec{j}_2\cdot\vec{j}_2 - 3j_{2z}^2) + c^{(3)}(\vec{j}_1\cdot\vec{j}_2 - 3j_{1z}j_{2z}) + \cdots\right\}$$

$$V_{\mu\mu}(\vec{R}) = \frac{1}{R^3}c_{\mu\mu}\sum_q (-1)^q C_{2,-q}(\theta,\phi)T_{2q}^{(2)}$$

Resonance identification

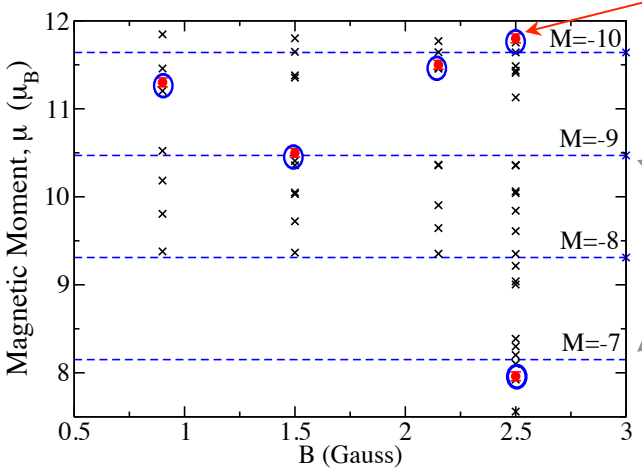

Experimental Magnetic moments

If we only include the isotropic C_6/R^6, rotation, and Zeeman interaction, the magnetic moments will be those of the atoms (gray lines).

Consequently, the observed variation of μ is a measure of the anisotropic interactions.

	B_{FR} (G)	μ^{exp}	μ^{calc}	R^* (a_0)	assignment $\lvert \ell, JM \rangle$
μ_1	0.9	11.3	11.20	72.0	$\lvert 4,\ 12\ -11/-10/-9\rangle$
	1.5	10.5	10.41	71.0	$\lvert 4,\ 12\ -8\rangle$
μ_2			10.36	71.0	$\lvert 4,\ 10\ -9\rangle$
μ_3	2.2	11.5	11.46	71.0	$\lvert 4,\ 10\ -10\rangle$
	2.5	11.8	11.75	86.0	$\lvert 2,\ 12\ -10\rangle$
μ_4	2.5	7.96	7.92	57.0	$\lvert 6,\ 10\ -7/-6\rangle$

It works rather well

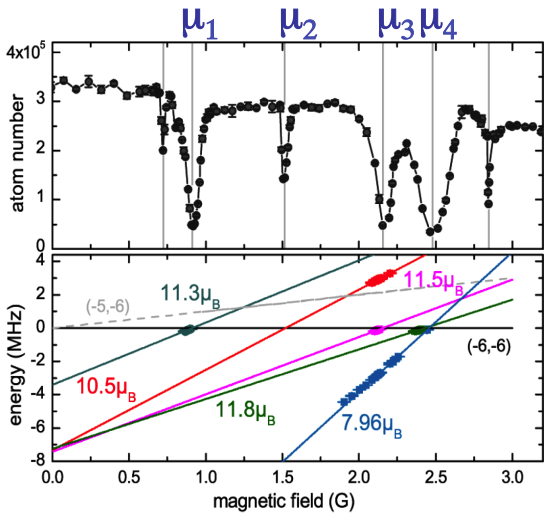

Atomic magnetic moments

Magnetic moments as a function of magnetic field strength.

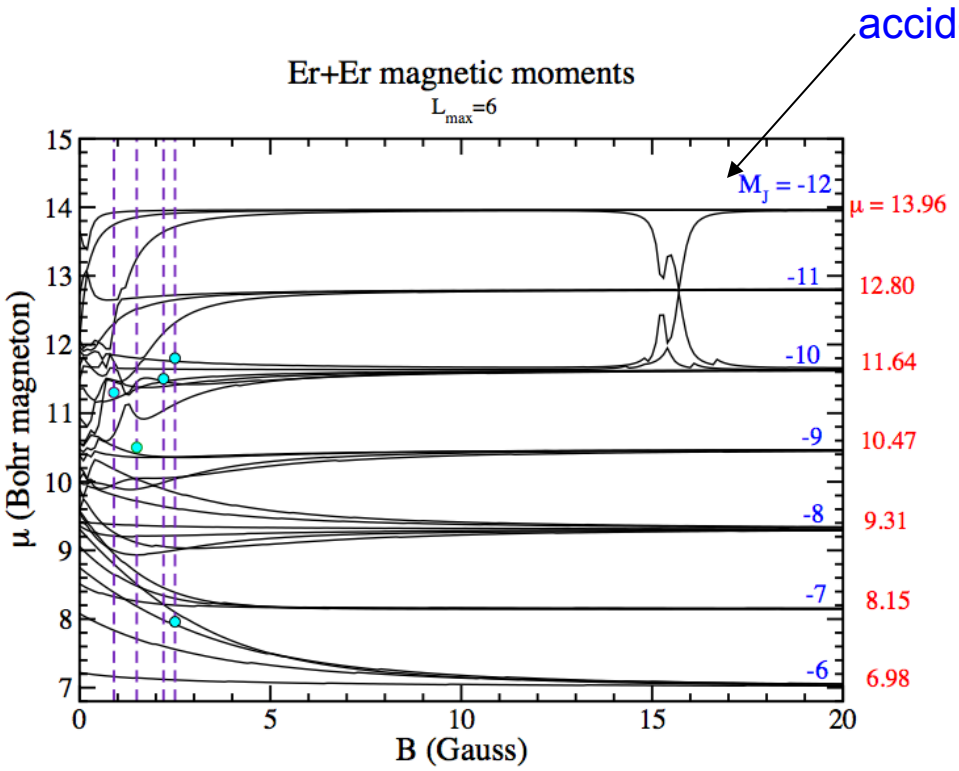

For large magnetic fields μ converges to the atomic value.

Highly magnetic molecules

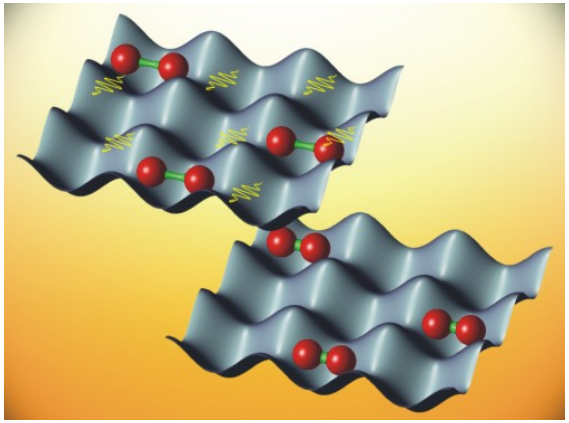

The interaction strength can be increased by up to four times by associating of two magnetic atoms into a molecule.

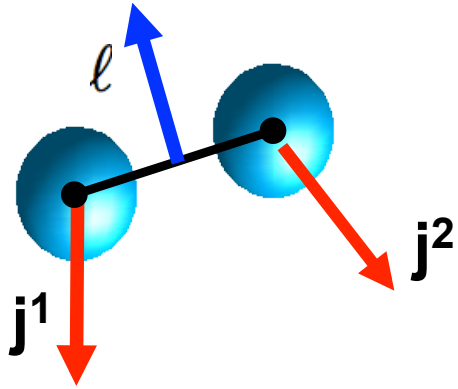

For Er_2, the maximum μ can be around 14 μ_B,

This corresponds to a dipolar length a_d = 1589 a_0, which is much larger than vdW length of 64 a_0.

Topics for the afternoon discussions

- Chaotic behavior of level (resonance) distribution in atomic/ molecular scattering vs scattering of many strongly interacting nucleons. (The sub mK energy physics of the ultracold against strongly coupled 1000 K energy physics).

- Applicability of effective-field theory to the high-spin atomic systems.

- How do two-body losses influence the three-body recombination rate?